European Journal of Pharmacology 764 (2015) 346–352

Contents lists available at ScienceDirect

European Journal of Pharmacology

journal homepage: www.elsevier.com/locate/ejphar

Molecular and cellular pharmacology

The pro-healing effect of exendin-4 on wounds produced by abrasion in normoglycemic mice

Stefano Bacci [a], Annunziatina Laurino [b], Maria Elena Manni [b], Elisa Landucci [c], Claudia Musilli [b], Gaetano De Siena [c], Alessandra Mocali [d], Laura Raimondi [b,*]

[a] Department of Clinical and Experimental Medicine, Research Unit of Histology and Embriology, University of Florence, 50139 Florence, Italy
[b] Department of NEUROFARBA, Section of Pharmacology, University of Florence, 50139 Florence, Italy
[c] Department of Health Sciences, Section of Pharmacology, University of Florence, 50139 Florence, Italy
[d] Department of Experimental and Clinical Biomedical Sciences, Section of Experimental Pathology and Oncology, University of Florence, 50134 Florence, Italy

ARTICLE INFO

Article history:
Received 28 April 2015
Received in revised form
25 June 2015
Accepted 26 June 2015
Available online 8 July 2015

Keywords:
Wound healing
Exendin-4
Exendin-4(9-39)
Angiogenesis
Glucagon-like type 1 receptor

ABSTRACT

Experimental evidence suggested that Exendin-4 (Exe4), an agonist at glucagon like receptor-1 (GLP-1R), promoted tissue regeneration. We aimed to verify the effect of Exe4, in the absence or in the presence of Exendin-4(9-39), an antagonist at GLP-1R, on the healing of abraded skin.

Two wounds (approximately 1.1 × 1.1 cm^2; namely "upper" and "lower" in respect of the head) were produced by abrasion on the back of 12 mice, which were then randomly assigned to receive an intradermal injection (20 μl) of

Group 1: saline (NT) or Exe4 (62 ng) in the upper and lower wound respectively;

Group 2: Exendin-4(9-39) (70 ng) in the upper and Exendin-4(9-39) (70 ng) and, after 15 min, Exe4 (62 ng) in the lower wound.

Wounds were measured at the time of abrasion (T0) and 144 h (T3) afterward taking pictures with a ruler and by using a software. The inflammatory cell infiltrate, fibroblasts/myofibroblasts, endothelial cells and GLP-1R expression, were each labeled by immunofluorescence in each wound, pERK1/2 was evaluated by Western-blot in wound lysates.

At T3, the percentage of healing surface was 53% and 92% for NT and Exe4 wounds respectively and 68% and 79% for those treated with Exendin-4(9-39) and Exendin-4(9-39)+Exe4 respectively. Exe4, but not Exendin-4(9-39) induced quantitative increase in fibroblasts/myofibroblasts and vessel density when compared to NT wounds. This increase was not evident in wounds treated with Exendin-4(9-39)+Exe4.

Exe4 promotes wound healing opening to the possible dermatological use of this incretin analogue.

1. Introduction

Exendin-4 (Exe4) is a natural peptide sharing 53% homology with Glucagon-like peptide-1 (GLP-1), the insulinotropic intestinal peptide belonging to the incretin hormones. Exe4 activates GLP-1 receptor (GLP-1R) thus mimicking most of GLP-1 effects including the ability to induce receptor phosphorylation and internalization (Roed et al., 2013), two mechanisms ensuring a continuous recycling from intracellular stores towards the plasma membrane (Widmann et al., 1995). Since the insulinotropic activity of GLP-1 was found dysregulated in diabetic patients (Meier and Nauck, 2010), a synthetic version of Exe4, exenatide, became recently part of an innovative anti-diabetic therapy (incretin analogues). The advantages for diabetic patients taking this drug include almost the null risk of experiencing hypoglycemia, the reduction of body weight gain, the protection against cardiovascular and neurological complications, the amelioration of foot ulcer healing and an improvement of psoriasis (He et al., 2013; Mannucci and Dicembrini, 2012; Drucker and Rosen 2011). Until now, it is unknown whether these effects are secondary to the correction of hyperglycemia or if they depend on activation of extra-pancreatic GLP-1R thus opening the possibility that Exe4 may have clinical usefulness beyond the correction of hyperglycemia.

Small chemical modifications on Exe4 primary structure produced Exendin-4(9-39), a peptide which is devoid of intrinsic activity at the GLP-1R (Al-Sabah et al., 2014) and consequently considered to be an antagonist. The binding of Exe4 and of

Abbreviations: GLP-1, Glucagon like peptide-1; GLP-1R, Glucagon like peptide-1 receptor; Exe4, Exendin-4

* Corresponding author. Fax: +39 0554271280.
E-mail address: laura.raimondi@unifi.it (L. Raimondi).

http://dx.doi.org/10.1016/j.ejphar.2015.06.056
0014-2999/

Exendin-4(9-39) at the GLP-1R would be mutually exclusive (Donnelly, 2012). Overall, Exe4 and Exendin-4(9-39), represent important experimental tools for investigating the pharmacology of GLP-1R.

Recent experimental evidence suggest a possible role for Exe4 in the promotion of tissue regeneration. It was reported that Exe4 was able to stimulate endothelial cell migration (Kang et al., 2013), to inhibit apoptosis (Favaro et al., 2012; Khang et al., 2013), and to reduce inflammation and oxidative stress in myocardial post-conditioning (Du et al., 2014) Interestingly, all these effects were prevented by Exendin-4(9-39).

We hypothesized a possible role for Exe4 in wound healing, a pro-survival event consisting of functionally distinct and temporally overlapping processes involving the coordinated activity of multiple cell types s, orchestrated by growth factors, cytokines and extracellular matrix components to avoid the chronicization of the wound and the risk of life treating sepsis (Gurtner et al., 2008; Schultz et al., 2011).

Since GLP-1R is expressed at mouse skin (List et al., 2006), we decided to investigate the differences, if any, of treating wounds by abrasion with saline (NT) or with a single high dose of peptides which interact at GLP-1R including Exe4, an agonist, Exendin-4(9-39), an antagonist or a combination of both.

2. Material and methods

2.1. Animals

Male mice (CD1 strain) from the Harlan lab (MI, Italy) were used. Five mice were housed per cage and placed in the experimental room 24 h before use. The animals were kept at 23 ± 1 °C with a 12 h light–dark cycle (light on at 07:00 h) and were fed a standard laboratory diet with water ad libitum. Experiments and animal use procedures were in accordance with the National Institutes of Health Guide for the Care and Use of Laboratory Animals (NIH Publications no. 80-23, revised 1996). The experimental protocols were approved by the Animal Care Committee of the Department of Pharmacology, University of Florence, in compliance with the European Convention for the Protection of Vertebrate Animals used for Experimental and Other Scientific Purposes (ETS no. 123) and the European Communities Council Directive of 24 November 1986 (86/609/EEC). The authors further attest that all efforts were made to minimize the number of animals used and their suffering.

2.2. Experimental protocol

Mice (35.33 ± 1.45 g body weight; means ± S.E.M of 12 mice) were anesthetized with a single intra-peritoneal injection of ketamine (80 mg/kg body weight)/xylazine (10 mg/kg body weight). After surgical anesthesia, the back of these mice was shaved and disinfected with 70% ethanol.

Two circular wounds (approximately 1.1 × 1.1 cm^2) at a distance of about 1 cm apart, were produced by one single researcher on the back of 12 animals, referred as “upper” and “lower” depending on their location with respect to the head of the mouse (see Fig. 1; Immonen et al., 2014). Dermabrasion was performed using commercial sandpaper (KWH Mirka Ltd., Jeppo, Finland; grain size 68 μm). The animals were exposed to dermabrasion for about 15 s until the complete removal of the epidermis but avoiding deep wounds. During the treatment the animals were kept on a bed at a constant temperature (37.5 °C) to reduce stress due to anesthesia. Immediately after, a small amount of Streptosil was applied topically to prevent the onset of infections. The wound was left uncovered during the whole period of experiments. All the animals

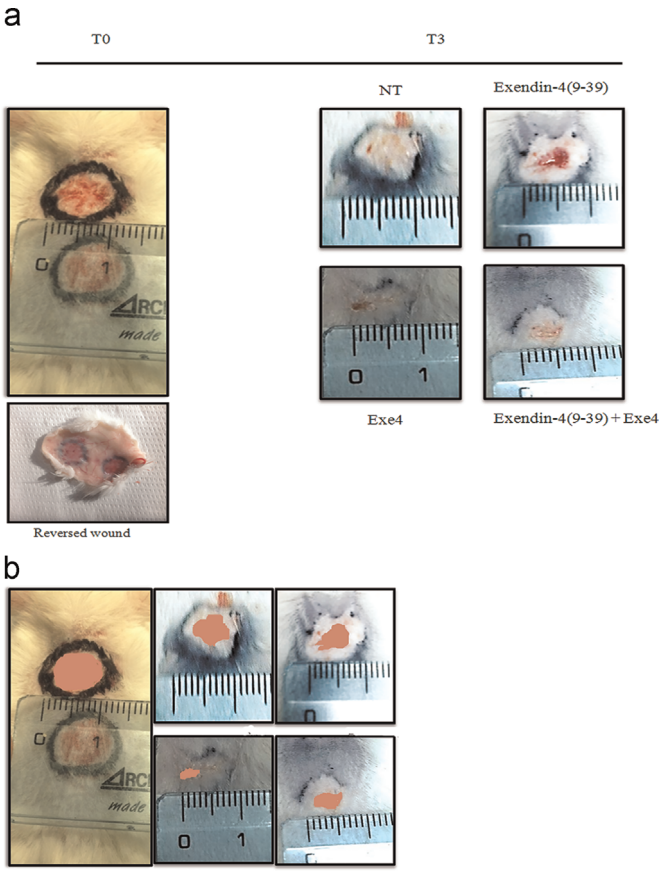

Fig. 1. The effect of treatment on wound healing. Wounds from abrasion were produced on the back of normoglycemic mice and injected intradermically with 20 μl of the drugs as described in Section 2. Panel A: pictures from mice after abrasion (T0) and at the end of the experiment (T3). Panel B: pictures of wounds from mice killed at T0 and T3 whose area was filled by a software (pixels).

were then housed individually to prevent traumatic damage to the wounds by other mice.

Another researcher was assigned to treat animals as it follows: mice were randomly divided in two groups and their wounds received the following treatments:

Group 1 ($n=6$): 20 μl of saline solution (NT) or of Exe4 (62 ng; Sigma-Aldrich, St. Louis, MO, USA) were injected in the dermis of the upper and the lower wound respectively;

Group 2 ($n=6$): 20 μl of Exe4(9-39) (Sigma-Aldrich, St. Louis, MO, USA) or Exe4(9-39) followed by 20 μl of Exe4 (62 ng; Sigma) after 15 min in the dermis of the upper and the lower wound respectively.

The intradermal route was chosen because the epithelium was discontinuous and inflamed after abrasion. The dose of Exe4 used (62 ng) was similar to that used by Du et al. (2014), it was within the safety range in rodents (FDA, Application no. 21-773) and it aimed to produce a drug reserve at the site of the injury. The presence of a small swelling at the injection site was taken as an indication that the treatment was performed successfully.

Two animals from both groups were killed by cervical dislocation at the time of abrasion (T0). Pictures were taken by using a ruler to measure the initial size of the wounds. The remaining animals from Group 1 and 2 ($n=4$) were killed 144 h (T3) after abrasion. Pictures were again taken using a ruler to measure the size of the wounds. The wounds removed always included the complete epithelial margins and the scab, when present. Each wound portion was codified and stored at −80 °C until used for biochemical and histological evaluations. All measurements were performed at the end of the experiment in blinded fashion by

researchers not involved in wound preparation and treatment.

2.3. Western-blot analysis

Wound biopsies were homogenized in lysis buffer of the following composition (in mM): 50 Tris–HCl (pH 7.5), 150 NaCl, 1 EDTA, 5 sodium pyrophosphate, 10 -glycerophosphate, 1 Na_3VO_4, 0.2 phenylmethylsulfonyl fluoride, 25 μg/ml leupeptin, 10 μg/ml aprotinin, 0.1% SDS. The homogenates were then centrifuged at 15,000*g* for 15 min at 4 °C and the supernatants were used for Western-blot analysis.. Twenty μg of protein lysate were separated on 10% SDS-PAGE and transferred to PVDF membranes (60 min at 400 mA) using standard procedures. The blots were incubated overnight at 4 °C with specific antibodies against pERK1/2 or actin (Santa Cruz Biotechonology, Dallas, TX, USA) diluted 1:1000 in TPBS (PBS added to 0.1% Tween) containing 1% serum bovine albumin. After being washed with TPBS, the PVDF membranes were incubated with polyclonal anti-rabbit or anti-mouse horseradish peroxidase-conjugated secondary antisera (1:100000 in PTBS containing 1% albumin; Sigma-Aldrich, St. Louis, MO, US) and left for 1 h at room temperature. The blots were then extensively washed and developed using an enhanced chemiluminescence detection system (Pierce, Italy). The exposure and developing time were standardized for all blots. Densitometric analysis of the scanned images was performed on a Macintosh iMac computer using the public domain NIH Image program. Protein concentration was quantified using the BCA method (Pierce, Italy).

2.4. Histology and histochemistry

For histological evaluations, the specimens were embedded in freezing tissue medium (Killik; BioOptica, Milan, Italy), and the cryosections were post fixed in cold acetone. Sections from each case (one section per staining) were stained with haematoxilin and eosin (HE) or labeled with the following antibodies: Ly6G for inflammatory cells ($Ly6G^+$; 1:50, Abnova, Tapei city, Taiwan), Hsp47 for fibroblasts ($Hsp47^+$; 1:75, Abcam, Cambridge, UK), Acta2 for myo-fibroblasts ($Acta2^+$; 1:100, Abnova), and CD31 for endothelial cells ($CD31^+$; 1:100, Abcam). Appropriate fluorescein isothiocyanate and/or rhodamine labeled polyclonal antibodies from rabbit or mouse (1:32; Sigma, Milan Italy) were used as secondary labels. The primary antibodies were applied overnight at 4 °C, and secondary ones were applied for 2 h at 37 °C. Omission of the primary antibody and substitution with an irrelevant one was used as a control for the immunohistochemical reactions. The sections were photographed using a Leitz optical microscope equipped with a camera and connected to a personal computer (LG), and the images were visualized with Progres Capture Basic software (Jenoptik, Jena, Germany) or a Zeiss Axioskop microscope suitable for epifluorescence and equipped with a digital photocamera (Zeiss), connected to a personal computer (ED, Rome, Italy) hosting Axiovision 4 software (Zeiss) or a Leica confocal microscopy TCS SP5, Wetz, Germany.

2.5. Morphometry

Cellular infiltration, as shown in haematoxilin and eosin (HE) stained sections, was graded on a 0–3 arbitrary scale for each biopsy site (Bonelli et al., 2003). Immunostained sections were placed one at a time on the microscopic stage; adjacent but not overlapping fields of the dermis were photographed separately, at ×40 magnification. Sections from each case (one section per staining) were stained and a minimum of ten microscopical fields were used for each sample. $Hsp47^+$, $Acta2^+$, $Ly6G^+$ were counted using the software image analysis Image J 1.37v (National Institutes of Health, Bethesda, MD) as follows. The background gray level was measured, the threshold was set at 1.5 times the background and the structures in the dermis that were brighter (i.e. more intensely fluorescent) than the threshold were counted by the software. The counts were obtained for spots larger than 50 pixels, which were assumed to represent whole cells. For each comparison, the average value for each specimen was measured as a sample unit. One photomicrograph from each specimen was taken from $CD31^+$ cells in sections; the area of vessels and that of the dermis were measured and the relative volume of surface vessels within the dermis was computed.

2.6. Statistical analysis

Data are presented as means ± S.E.M. The statistical significance of differences was determined by Student's t tests or the ANOVA test using the StatView 512+ program (Abacus Concepts, Berkeley, CA) (Bacci et al., 2014). A value of $P<0.05$ was considered statistically significant.

3. Results

3.1. The effect of treatments on wound closure

The wounds had an initial mean area of 0.95 ± 0.1 cm^2 (Fig. 1, panel A), calculated with the assumption that the wounds were a circle of 1.1 ± 0.1 cm in diameter. The size of the wounds, including the absence of new hair growth and signs of the initial abrasion (excluding healed surface areas), was re-evaluated after 6 days (T3) to assess the effect of the treatments on the healing process taking pictures of the wounds with a ruler (extrapolating that the wounds were circular in shape and considering the highest axes) (Fig.1, panel B) or by using a software. Both methods gave similar results which were reported in Table 1.

Accordingly, after de-codification of the biopsyes, it resulted that the wounds treated with NT and Exe4 healed up to 53% and 92–90% respectively of their initial size. Exendin-4(9-39) treatment did not modify the spontaneous healing process (68–69% vs. 53–45% in NT). Instead, the presence of Exendin-4(9-39) reduced the effect of Exe4 causing 79–76% of the surface to be healed.

At the time of the sacrifice, mice from Group 1 and 2 weighed (g) 35.66 ± 1.76 and 37.0 ± 1.0 respectively ($n=8$) thus indicating they did not lose weight during the experiment. Furthermore, the animals never presented diarrhea.

From this macroscopic evidence, we decided to characterize some of the indicators of healing by immunoistochemical and biochemical approaches in wounds collected at different times after abrasion.

Table 1
The effect of treatments on the healing of wounds by abrasion.

Treatments	*Unhealed Surface* (cm^2)	*Healed* (%)	*Unhealed Surface* (pixels)	*Healed* (%)
NT	0.50 ± 0.07	53	3485 ± 180	45
Exe4	0.07 ± 0.02[a]	92	633 ± 55[a]	90
Exendin-4(9-39)	0.30 ± 0.05	68	2295 ± 130	63
Exendin-4(9-39)+Exe4	0.2 ± 0.04[b]	79	1502 ± 68[a,c]	76

Wounds were produced and treated as described in Section 2. When produced, wounds measured 0.95 ± 0.1 cm^2 or 6360 pixels. At T3, the percentage of the healed surface was calculated referring to the initial size of the wounds (cm^2 or pixels). Results reported in cm^2 were calculated extrapolating the unhealed surface to a circle considering the longest axis. Results reported in pixels were calculated by using a software and the number of pixels were reported ($n=4$). The symbols a, b and c mean $P<0.01$ and $P<0.1$ vs. NT and $P<0.5$ vs. Exe4 respectively.

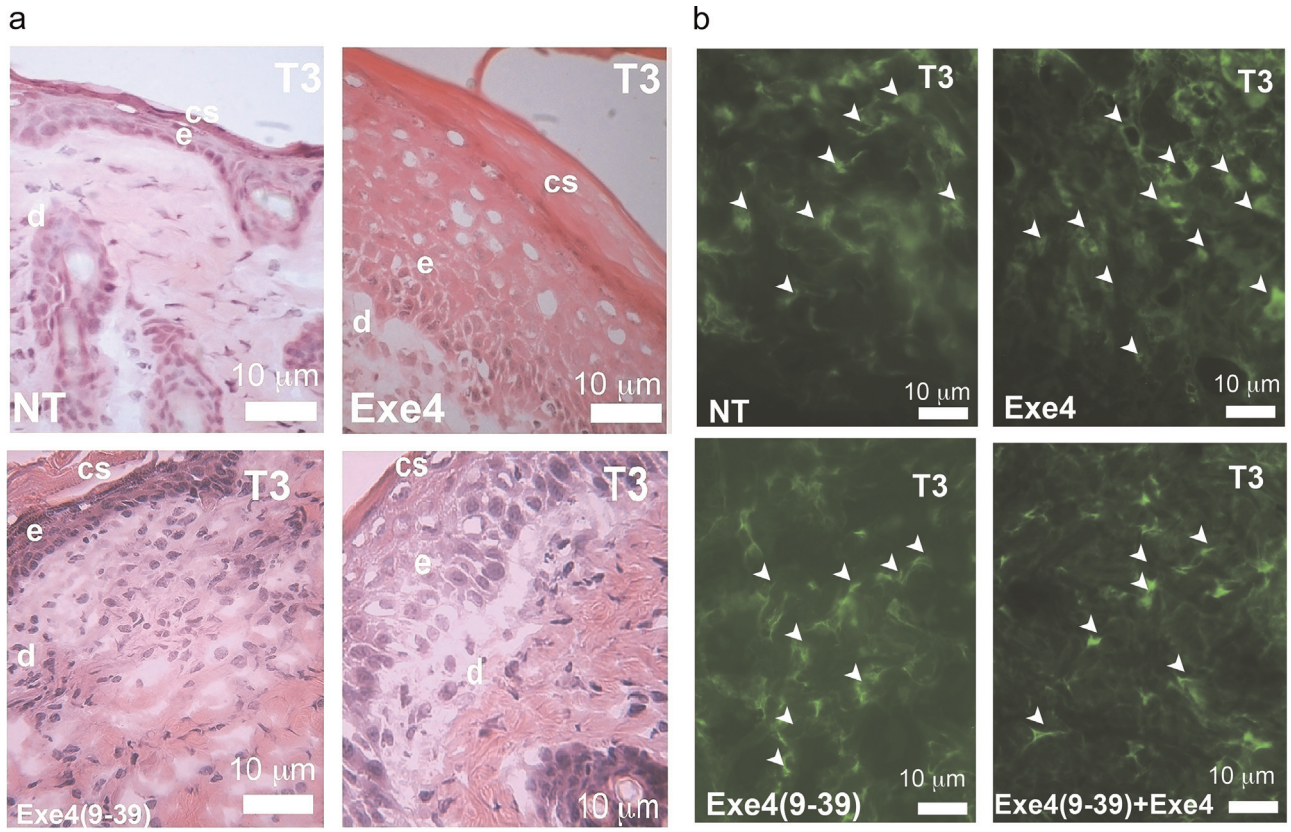

Fig. 2. Evaluation of the inflammatory infiltrate in the wounds: the effect of treatments. The inflammatory infiltrate was evaluated as described in Section 2 by haematoxilin eosin (HE) and by Ly6g$^+$ staining Panels A: HE staining of wounds; cs=corneum stratum; e=epithelial layer; d=dermis. Panels B and d: Ly6G$^+$ staining as described in Section 2; arrows indicates Ly6G$^+$ cells.

3.2. Inflammatory infiltration of the wounds

We then assessed the effect of the treatments on the the inflammatory cell infiltrate by Hematoxilin Eosin (HE) (Fig. 2, panel A), by immunostaining of Ly6G$^+$ (Fig. 2, panel B). Analysis from HE indicated the presence of similar extent of inflammatory cell infiltrate (2.36 ± 0.21, 2.43 ± 0.17, 2.33 ± 0.27, 1.21 ± 0.11 in NT, Exe4, Exendin-4(9-39) and Exendin-4(9-39)+Exe4 respectively) and also the presence of a corneum stratum in all the wounds irrespective of the treatment received.

3.3. Exe4 promotes fibroblast accumulation and their differentiation into myofibroblasts

Fibroblasts were labeled by measuring the expression of HSP47, and their number was evaluated as described in Section 2. The fibroblast number was high in wounds received NT, and Exendin-4 (9-39) (Fig. 3, panel A). However, in Exe4, this number was significantly higher than with the other treatments (Fig. 3, panel A and B) in wounds received Exendin-4(9-39)+Exe4, the number of Hsp47$^+$ cells were significantly lower than in all the other experimental conditions (Fig. 3, panel A).

The differentiation of fibroblasts into myofibroblasts is an essential event leading to the contraction of the wound (Hinz, 2010). Immunohistochemical analysis revealed the presence of rare Acta2$^+$ cells in NT and Exendin-4(9-39) wounds (data not shown). Instead, in wounds treated with Exe4, Acta2$^+$ cells represented 23% of fibroblast population. This percentage decreased to 6% and 3% in Exendin-4(9-39) and Exendin-4(9-39)+Exe4 treated wounds respectively (Fig. 3, panels A, B, and C).

Interestingly, myofibroblasts were positive for immunostaining of GLP-1R both at the cell membrane and in the cytoplasm (Fig. 3, panel D).

3.4. Exe4 treated wounds present ERK1/2 activation

Activation of pERK was recognized as a downstream event to GLP-1R activation (Favaro et al., 2012). To verify whether activation of the kinase was also evident at our experimental settings and if it was modulated by Exe4 and Exendin-4(9-39), we evaluated pERK1/2 levels in our wounds specimens. Our results indicated that, ERK1/2 was found indeed found activated at T3 in Exe4 treated wounds. At the same time point, ERK1/2 activation was not evident in wounds receiving NT or those treated with Exendin-4 (9-39)+Exe4 (Fig. 4).

3.5. Exe4 promotes endothelial cell proliferation

In NT and Exendin-4(9-39) treated wounds, few CD31$^+$ cells were detected (Fig. 5, panel A). In Exe-4 treated wounds, the number of CD31$^+$ cells was higher than in NT and Exendin-4(9-39). Again, CD31$^+$ cells were significantly lower in Exendin-4(9-39)+Exe4 treated wounds than in all the other wounds (Fig. 5, panels A and B).

4. Discussion

We here provide evidence demonstrating that an high dose of Exe4, but not of Exendin-4(9-39), quantitatively modifies the morphology of regenerating mouse skin. In particular, treating wounds by abrasion with Exe4 produces a significant increase of vessel density, fibroblast migration and differentiation in respect of that produced by a saline treatment. These changes might

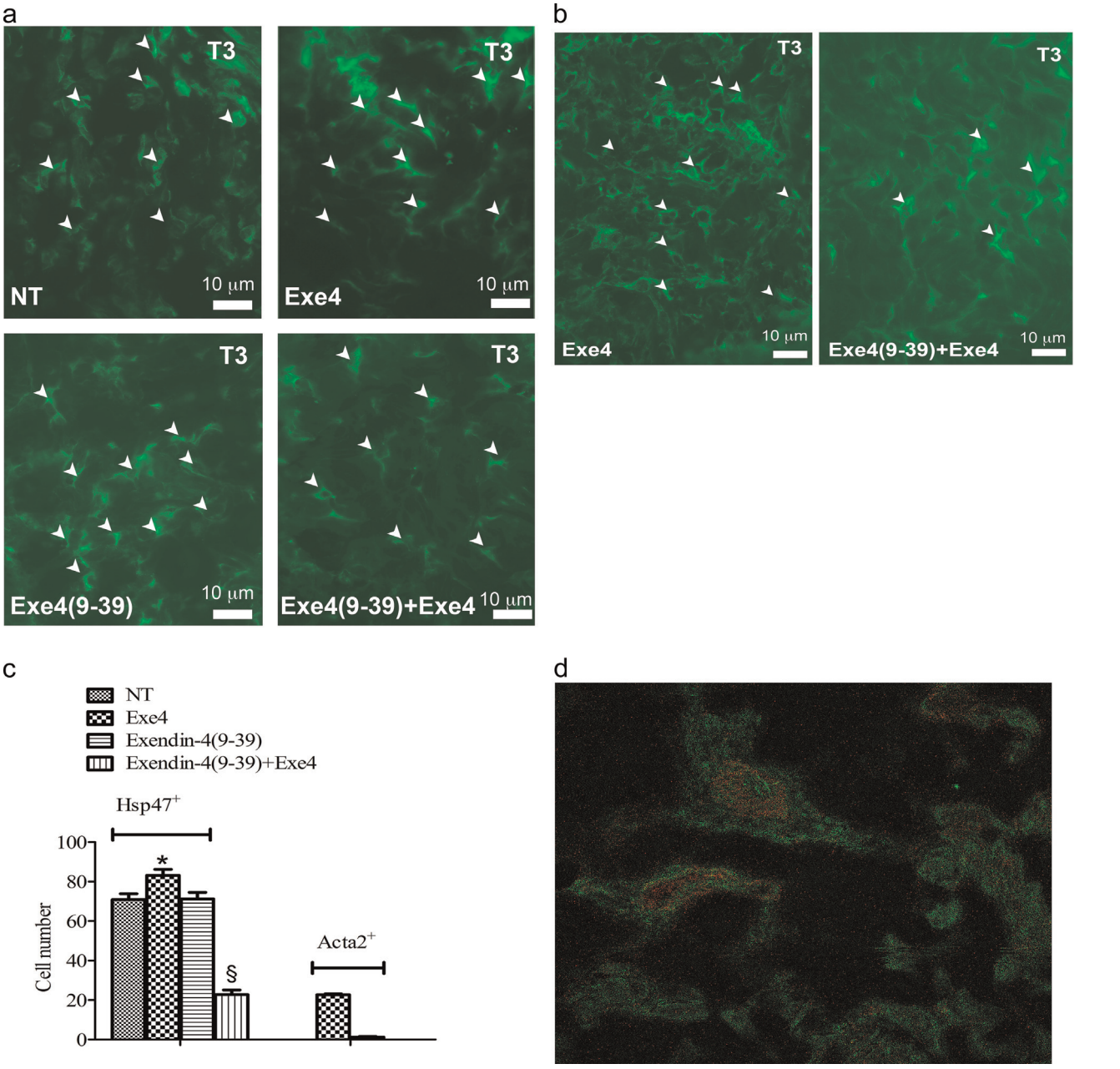

Fig. 3. The effect of treatment on fibroblast/myofibroblast number at the site of the wound and GLP-1R expression at myofibroblasts. Fibroblasts and myofibroblasts, GLP-1R were each labeled by immunofluorescence as described in Section 2 Panel A: in wounds collected at T3 and counted (10 microscopic field) as described in Section 2 Arrows indicates HSP47$^+$ cells. Panel B: myofibroblasts were evaluated. Arrows indicates Acta2$^+$ cells. Panel C: Densitometric analysis of data was performed as described in Section 2 Panel D: a pictures showing myofibroblasts positive for GLP-1R, a double immunostaining.

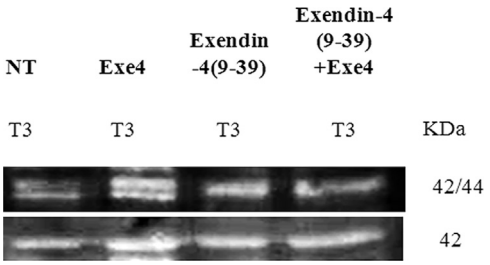

Fig. 4. The effect of treatments on the levels of pERK1/2. Western blot analysis for pERK1/2 in wounds collected at different times was performed as described in the Section 2. pERK1/2 level of expression was evaluated in in wounds treated with NT, Exe4, exendin-4(9-39) and Exendin-4(9-39)+Exe4. A typical experiment is shown.

account for the finding indicating that, after 6 days, the wounds received Exe4 were more healed than those treated with NT, exendin-4(9-39) but also with Exendin-4(9-39)+Exe4. Furthermore, we found, in line with that already described by Ishibashi et al. (2011), myofibroblasts positive for GLP-1R immunostaining both at the plasma membrane and intracellular (Widmann et al., 1995; Roed et al., 2013). In addition, activation of the mitogenic ERK1/2, was described as part of the intracellular cascade activated by GLP-1R (Favaro et al., 2012). Accordingly with this and with the occurrence of a regenerating process, our results show that in wounds treated with Exe4, activation of ERK1/2 was found. Interestingly, this activation was not observed in lysates from wounds treated with Exendin-4(9-39)+Exe4, thus indicating that

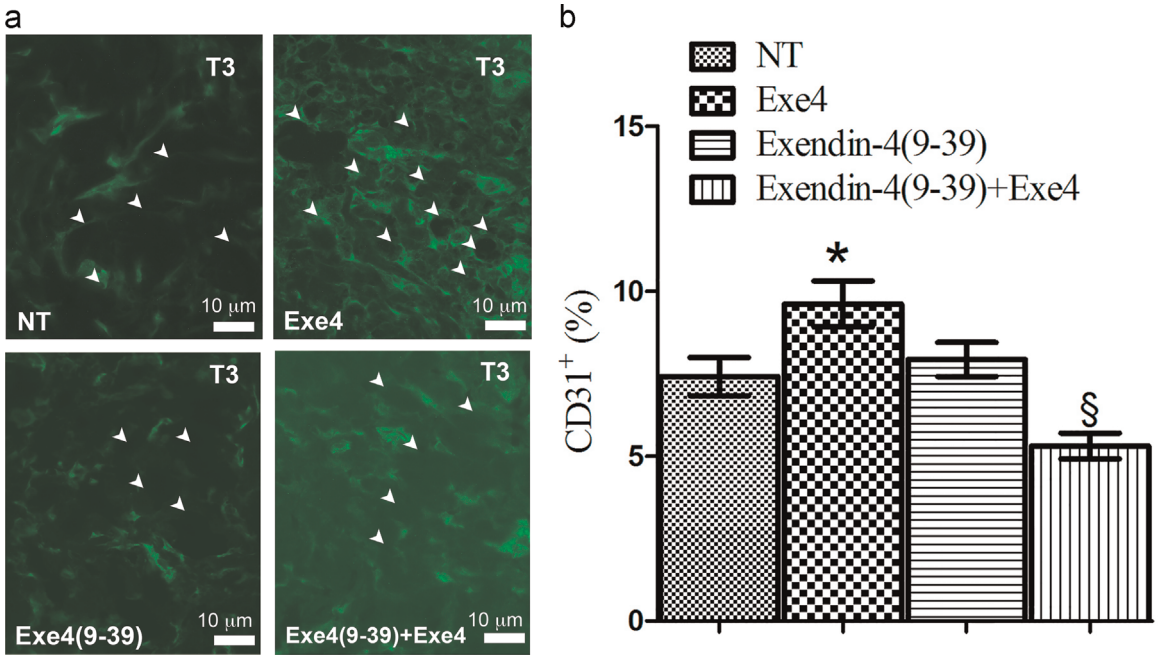

Fig. 5. The effect of treatments on the number of endothelial cells. The number of endothelial cells in wounds were evaluated (at least ten microscopic filed for section) as described in Section 2 in wounds collected at T3. Panel A: arrows indicates $CD31^+$ cells. Panel B: endothelial cell number was evaluated as described in Section 2 $^*P < 0.05$ vs. NT; §$P < 0.05$ vs. Exe4.

the kinase is somehow related to GLP-1R activation.

All together these results allow to hypothesize that activation of GLP-1R is the determinant of beneficial effects of Exe4 on wound repair. Of course, due to the high dose of Exe4 used, effects of the peptide independent of GLP-1R activation cannot be excluded but, if any, they were not recognized at our settings.

Exe4 has been reported to exert anti-inflammatory and anti-oxidative but also pro-angiogenic effects in different experimental pathological settings (Cechin, et al., 2012;. Lee et al., 2012; Kang et al., 2013) characterized by an high oxidative status. Actually, we did not find any significant differences induced by treatments in the inflammatory infiltration of wounds, at least at our point of observation. Of course, we cannot exclude different results at earlier time of observations. Instead, according to the literature, we found higher fibroblasts/myofibroblasts and endothelial cells in Exe4 than in NT and Exendin-4(9-39) treated wounds. To note, when both Exe4 and Exendin-4(9-39) were present, the number of fibro/myfibroblasts recovered in the wounds were significantly lower than with NT treatment. The reason of such result is unknown yet and several hypothesis can be drawn including modifications of the pharmacokinetic and pharmacodymanic features of each peptide and, more likely, a different kinetic of activation/deactivation of fibroblast occurrence when both peptides were used.

From our data it appears that the pharmacological application of Exe4 "accelerates" the healing of wounds from abrasion in an experimental model where the healing process is not compromised by pre-existing pathologies. Even if the molecular event (s) triggered by Exe4 remain(s) to be identified, we have described morphological changes of mouse skin promoted by Exe4 and prevented by the presence of Exendin-4(9-39), findings suggesting the involvement of GLP-1R cascade activation.

The extra-pancreatic actions of Exe4 are a broad and expanding topic of interest. In this respect, our results potentially expand the utility of Exe4 to the treatment of dermatological diseases, including skin wound healing.

4.1. Study limitations

This study has several limitations, including the high dose of Exe4 used and our lack of knowledge of the molecular cascade activated by Exe4. As already stated, Exe4 dose was chosen to avoid daily medication of the wounds and because we did not know if Exe4 had any bioavailability at the skin following its normal subcutaneous route of administration. Of course, we cannot exclude that Exe4 could have some systemic bioavailability when given intradermal or that a "cross" drug contamination between the "upper" and the "lower" wounds may occur. However, both situations seem be not relevant for the interpretation of results since collateral effects in including diahorrea were not evident (Di Pasquale et al., 2012) and significant differences among the effects of treatments were nonetheless appreciated.

Acknowledgments

Financial support was granted by a localgrant from the University of Florence and by the Ente Cassa di Risparmio di Firenze (Grant no. 3681 to S.B.).

We thank Nadia Trevisan for helping us with animal housing.

References

Al-Sabah, S., Al-Fulaij, M., Ahmed, H.A., 2014. Selectivity of peptide ligands for the human incretin receptors expressed in HEK-293 cells. Eur. J. Pharmacol. 741, 311–315.

Bacci, S., De Fraia, B., Cinci, L., Calosi, L., Guasti, D., Pieri, L., Lotti, V., Bonelli, A., Romagnoli, P., 2014. Immunohistochemical analysis of dendritic cells in skin lesions: correlations with survival time. Forensic Sci. Int. 244, 179–185.

Bonelli, A., Bacci, S., Norelli, G.A., 2003. Affinity cytochemistry analysis of mast cells in skin lesions: a possible tool to assess timing of lesions toward death. Int. J. Leg. Med. 117, 331–334.

Cechin, S.R., Pérez-Álvarez, I., Fenjves, E., Molano, R.D., Pileggi, A., Berggren, P.O., Ricordi, C., Pastori, R.L., 2012. Anti-inflammatory properties of exenatide in human pancreatic islets. Cell Transplant. 21, 633–648.

Di Pasquale, G., Dicembrini, I., Raimondi, L., Pagano, C., Egan, J.M., Cozzi, A., Cinci, L., Loreto, A., Manni, M.E., Berretti, S., Morell, iA., Zheng, C., Michaell, D.G., Maggi,

M., Vettor, R., Chiorini, J.A., Mannucci, E., Rotella, C.M., 2012. Sustained exendin-4 secretion through gene therapy targeting salivary glands in two different rodent models of obesity/type 2 diabetes. PLos One 7, e40074.
Donnelly, D., 2012. The structure and function of the glucagon-like peptide-1 receptor and its ligands. Br. J. Pharmacol. 166, 27–41.
Du, X., Hu, X., Wei, J., 2014. Anti-inflammatory effect of exendin-4 postconditioning during myocardial ischemia and reperfusion. Mol. Biol. Rep. 41, 3853–3857.
Drucker, D.J., Rosen, C.F., 2011. Glucagon-like peptide-1 (GLP-1) receptor agonists, obesity and psoriasis: diabetes meets dermatology. Diabetologia 54, 2741–2744.
Favaro, E., Granata, R., Miceli, I., Baragli, A., Settanni, F., Cavallo Perin, P., Ghigo, E., Camussi, G., Zanone, M.M., 2012. The ghrelin gene products and exendin-4 promote survival of human pancreatic islet endothelial cells in hyperglycaemic conditions, through phosphoinositide 3-kinase/Akt, extracellular signal-related kinase (ERK)1/2 and cAMP/protein kinase A (PKA) signalling pathways. Diabetologia 55, 1058–1070.
Gurtner, G.C., Werner, S., Barrandon, Y., Longaker, M.T., 2008. Wound repair and regeneration. Nature 453, 314–321.
He, L., Wong, C.K., Cheung, K.K., Yau, H.C., Fu, A., Zhao, H.L., Leung, K.M., Kong, A.P., Wong, G.W., Chan, P.K., Xu, G., Chan, J.C., 2013. Anti-inflammatory effects of exendin-4, a glucagon-like peptide-1 analog, on human peripheral lymphocytes in patients with type 2 diabetes. J. Diabetes Investig. 4, 382–392.
Hinz, B., 2010. The myofibroblast: paradigm for a mechanically active cell. J. Biomech. 43, 146–155.
Immonen, J.A., Zagon, I.S., McLaughlin, P.J., 2014. Topical naltrexone as treatment for type 2 diabetic cutaneous wounds. Adv. Wound Care 3, 419–427.
Ishibashi, Y., Nishino, Y., Matsui, T., Takeuchi, M., Yamagishi, S., 2011. Glucagon-like peptide-1 suppresses advanced glycation end product-induced monocyte chemoattractant protein-1 expression in mesangial cells by reducing advanced glycation end product receptor level. Metabolism 60, 1271–1277.
Kang, H.M., Kang, Y., Chun, H.J., Jeong, J.W., Park, C., 2013. Evaluation of the in vitro and in vivo angiogenic effects of exendin-4. Biochem. Biophys. Res. Commun. 434, 150–154.
Lee, J., Hong, S.W., Chae, S.W., Kim, D.H., Choi, J.H., Bae, J.C., Park, S.E., Rhee, E.J., Park, C.Y., Oh, K.W., Park, S.W., Kim, S.W., Lee, W.Y., 2012. Exendin-4 improves steatohepatitis by increasing Sirt1 expression in high-fat diet-induced obese C57BL/6J mice. PLoS One 7, e31394.
List, J.F., He, H., Joel, F., 2006. Habener Glucagon-like peptide-1 receptor and proglucagon expression in mouse skin. Regul. Pept. 134, 149–157.
Mannucci, E., Dicembrini, I., 2012. Incretin-based therapies and cardiovascular risk. Curr. Med. Res. Opin. 28, 715–721.
Meier, J.J., Nauck, M.A., 2011. Is the diminished incretin effect in type 2 diabetes just an epi-phenomenon of impaired beta-cell function. Diabetes 59, 1117–1125.
Roed, S.N., Wismann, P., Underwood, C.R., Kulahin, N., Iversen, H., Cappelen, K.A., Schäffer, L., Lehtonen, J., Hecksher-Soerensen, J., Secher, A., Mathiesen, J.M., Bräuner-Osborne, H., Whistler, J.L., Knudsen, S.M., Waldhoer, M., 2013. Real-time trafficking and signaling of the glucagon-like peptide-1 receptor. Mol. Cell. Endocrinol. 382, 938–949.
Schultz, G.S., Davidson, J.M., Kirsner, R.S., Bornstein, P., Herman, I.M., 2011. Dynamic reciprocity in the wound microenvironment. Wound Repair Regen. 19, 34–148.
Widmann, C., Dolci, W., Thorens, B., 1995. Agonist-induced internalization and recycling of the glucagon-like peptide-1 receptor in transfected fibroblasts and in insulinomas. Biochem. J. 310, 203–214.